European Cells and Materials Vol. 24 2012 (pages 107-117) DOI: 10.22203/eCM.v024a08 ISSN 1473-2262

FGF18 AUGMENTS OSSEOINTEGRATION OF INTRA-MEDULLARY IMPLANTS IN OSTEOPENIC FGFR3$^{-/-}$ MICE

A. Carli[1,2], C. Gao[1,3], M. Khayyat-Kholghi[1], A. Li[1], H. Wang[1], C. Ladel[4], E.J. Harvey[1,2] and J.E. Henderson[1,2,3,*]

[1]Bone Engineering Labs, Research Institute-McGill University Health Centre, Montreal, Qc, Canada
[2] Division of Orthopaedic Surgery, Department. of Surgery, McGill University, Montreal, Qc, Canada
[3] Division of Experimental Medicine, Department. of Medicine, McGill University, Montreal, Qc, Canada
[4] Merck Serono International SA, Geneva, Switzerland

Abstract

Enhancement of endogenous bone regeneration is a priority for integration of joint replacement hardware with host bone for stable fixation of the prosthesis. Fibroblast Growth Factor (FGF) 18 regulates skeletal development and could therefore have applications for bone regeneration and skeletal repair. This study was designed to determine if treatment with FGF 18 would promote bone regeneration and integration of orthopedic hardware in FGF receptor 3 deficient (FGFR3$^{-/-}$) mice, previously characterized with impaired bone formation. Rigid nylon rods coated with 200 nm of titanium were implanted bilaterally in the femora of adult FGFR3$^{-/-}$ and FGFR3$^{+/+}$ mice to mimic human orthopedic hardware. At the time of surgery, LEFT femora received an intramedullary injection of 0.5 μg FGF18 (Merck Serono) and RIGHT femora received PBS as a control. Treatment with FGF18 resulted in a significant increase in peri-implant bone formation in both FGFR3$^{+/+}$ and FGFR3$^{-/-}$ mice, with the peri-implant fibrous tissue frequently seen in FGFR3$^{-/-}$ mice being largely replaced by bone. The results of this pre-clinical study support the conjecture that FGF18 could be used in the clinical setting to promote integration of orthopedic hardware in poor quality bone.

Keywords: FGF18; FGFR3-/- mice; bone quality; bone regeneration; implant fixation.

*Address for correspondence:
J.E. Henderson
Division of Orthopaedic Surgery
Department. of Surgery
C9.133 Montreal General Hospital
1650 Cedar Ave, Montreal, Quebec,
Canada H3G 1A4
E-mail: janet.henderson@mcgill.ca

Introduction

The success of orthopedic procedures like joint replacement is critically dependent on bone regeneration for the stable fixation and integration of metal implants in host bone. The process referred to as osseointegration forms a living, functional interface between tissue and implant that provides a more rigid fixation, which reduces pain and permits earlier mobility and function (Junker *et al.*, 2009). Bone regenerative capacity decreases with increasing age and is impaired in younger individuals who have received medical treatment for chronic disease or cancer. The fixation of orthopedic hardware in these people is associated with a clinical failure rate that has been reported to be as high as 50 % (Nauth *et al.*, 2011). Pre-clinical studies have shown defective osteogenesis and bone mineralization, leading to poor fixation and implant integration, may be the main culprits for these poor clinical outcomes (Egermann *et al.*, 2005; Gao *et al.*, 2012).

Murine models that involve targeted mutation of genes encoding known regulators of skeletal development have been informative in revealing the growth factor signaling pathways that are necessary for adult bone metabolism and the induction of bone formation required for implant fixation. Targeted mutagenesis of fibroblast growth factor receptor 3 (FGFR3), which is one of four high affinity receptors for the 22 structurally related FGF ligands, resulted in overgrowth of the axial and appendicular skeleton in utero (Colvin *et al.*, 1996; Liu *et al.*, 2002) as well as osteomalacia, osteopenia and osteoarthritis in skeletally mature mice (Valverde-Franco *et al.* 2004; Valverde-Franco *et al.*, 2006). The FGFR3c isoform was later shown to be responsible for these skeletal defects (Eswarakumar and Schlessinger, 2007). Adult FGFR3$^{-/-}$ mice were thus shown to exhibit skeletal defects similar to those seen in the aging human skeleton and their mesenchymal stem cells (MSC) to exhibit atypical proliferation and differentiation compared to wild type control cells (Davidson *et al.*, 2005).

Of the ligands that bind to FGFR3, FGF 18 has been identified as playing a significant role in skeletal development. Activation of FGFR3 by FGF18 was shown to stimulate the proliferation and deposition of extracellular matrix by chondrogenic cells *in vivo* (Liu *et al.*, 2007) and *ex vivo* (Davidson *et al.*, 2005) and to increase *de novo* cartilage formation in a rat meniscal tear model (Moore *et al.*, 2005). In addition to its role in promoting cartilage regeneration and repair, FGF18 has also been implicated in bone formation. The phenotype of mice homozygous for targeted inactivation of FGF18

included delayed intramembranous bone formation that was not seen in mice lacking FGFR3 (Liu *et al.*, 2002), which predicts the effect was mediated through another FGFR. FGF18 could also influence bone growth through a pathway that recapitulates the ontogeny of endochondral ossification, by first stimulating chondrocyte proliferation and cartilage formation then regulating osteoblastogenesis. The osteogenic role for FGF18 suggests it might represent a potential therapeutic intervention to promote bone regeneration and osseointegration of orthopedic hardware in patients with poor bone quality. The objective of the current study was to examine the effect of local delivery of recombinant FGF18 on bone regeneration and fixation of a biocompatible implant in the femur of osteopenic $FGFR^{-/-}$ mice using $FGFR^{+/+}$ mice as control.

Materials and Methods

Implant fabrication

0.4 mm diameter nylon fishing line (Pure Fishing 1900, Spirit Lake, IA, USA) was cleaned by sonication for 30 min in 1 % : 1 % Renuzyme (Getinge, Getinge, Sweden) and Liqui-Nox (Alconox, White Plains, NY, USA) at 50 °C then in 2 % NaOH at 21 °C. After rinsing three times with distilled water at room temperature the line was placed in a vacuum oven and subjected to additional cleaning with high-pressure oxygen plasma etching. A uniform 200 nm layer of commercial grade pure titanium was deposited on the line using physical vapor deposition at the McGill Institute for Advanced Materials (http://www.mcgill.ca/miam/; Hacking *et al*., 2007). The titanium-coated lines were cut to 5 mm lengths before being placed in an aseptic environment under UV illumination, immersed in 70 % ethanol and rinsed three times with sterile phosphate-buffered saline (PBS).

Local FGF 18 administration and placement of implants in femoral canal

The mice used for this study were obtained from in-house breeding of $FGFR3^{+/-}$ mice obtained as a gift from D.M. Ornitz (Washington University, Seattle, WA, USA) and maintained for more than 30 generations on a C3H background. All procedures were performed in strict accordance with protocols approved by the McGill University Facility Animal Care Committee (FACC), based on guidelines set by the Canadian Council on Animal Care. Five $FGFR3^{+/+}$ and nine $FGFR3^{-/-}$ male mice aged 8 to 10 months were subjected to bilateral intramedullary implant surgery. After shaving the hindquarters, mice were anesthetized with inhaled vaporized isoflurane and bilateral 5 mm skin incisions made over the proximal hip to expose the greater trochanter and proximal femoral metaphysis. To access the intramedullary canal a 25-gauge needle was inserted medial to the greater trochanter, through the trochanteric notch, in a direction parallel to the femoral diaphysis. After removing the needle, 10 µL of sterile PBS containing 0.5 µg of recombinant human FGF18 (MW = 19.83 KDa, courtesy Merck Serono, Geneva, Switzerland) was injected into the LEFT canal, and PBS alone into the RIGHT canal, using a Hamilton syringe (Hamilton Company, Reno, NV, USA). After waiting 1 min for the solution to disperse a titanium-coated implant was inserted into each canal and the overlying muscle and skin re-apposed using 5-0 resorbable Vicryl sutures. All mice received subcutaneous analgesia immediately following surgery and for the first three postoperative days. Mice were allowed free access to food and water for six weeks postoperative before being euthanized and their femora harvested for analyses. Freshly isolated femora were dissected free of soft tissue and trimmed proximal to the condyles to allow permeation of the fixative (4 % paraformaldehyde) for 24 h and thorough washing with PBS for 48 h.

Micro CT analysis of peri-implant bone regeneration

Micro computed tomography (micro CT) was used to quantify bone regeneration around the implants using a Skyscan1172 instrument equipped with a 10 Mp camera (Skyscan, Kontich, Belgium). Using an energy source of 80 kV and 100 µA, images were captured at a rotation step of 0.45º between frames using a 0.5 mm aluminum filter resulting in a pixel size of 5 µm. Serial two-dimensional cross sections were assembled into 3D reconstructions and analyzed using Skyscan software, CTAn version 2.0.0.1, supplied with the instrument. Peri-implant tissue was quantified in a tubular region of interest (ROI) in the proximal metaphysis of the femur extending 30 µm out from the implant and 2 mm down from the lesser trochanter, which corresponds to the region measured previously in this model (Gao *et al*., 2012). A threshold of 40 % of the maximal possible grayscale value (80/200) was used to segment bone from non-bone tissue. Morphometric indices of bone volume and trabecular connectivity selected for representation from the binarized 3-dimernsional volume of interest included the ratio of bone volume to tissue volume (BV/TV), the number of trabeculae (TbN), the intersection surface (IntSu) that quantifies the amount of bone apposed to the implant and the structure model index (SMI), which compares the number of plate-like to rod-like trabeculae.

Histological analysis of peri-implant bone regeneration

After micro computed tomography (CT) analysis the femora were processed for embedding at low temperature in polymethylmethacrylate (PMMA) as described (Valverde-Franco *et al.*, 2004). Briefly, specimens were dehydrated in graded alcohols from 70 % to 100 % before vacuum infiltration and embedding in resin. 5 µm sections were cut in the proximal metaphyseal ROI using a modified Leica RM2265 rotary microtome (Leica Microsystems, Richmond Hill, Canada) and stained with 5 % silver nitrate for 30 min under ultraviolet light, then with 0.2 % toluidine blue for 1 min, to distinguish mineralized from un-mineralized tissue. Osteoblasts were identified by staining for alkaline phosphatase (ALP) and osteoclasts by staining for tartrate resistant acid phosphatase (TRAP) enzyme activity. Digital images were captured at x10 and x20 magnification using an Axioskop 40 equipped with an AxioCam MRc camera (Carl Zeiss Canada, Quebec, Canada) and compared with 2D axial micro CT images from the same region.

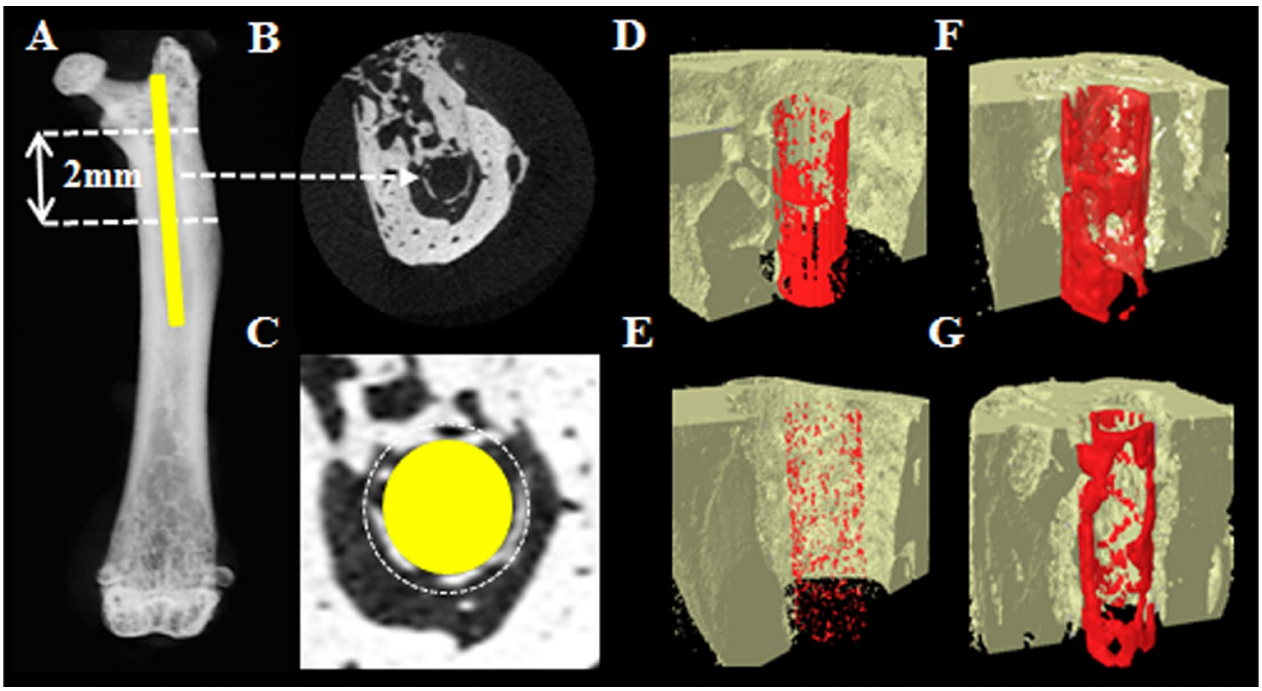

Fig. 1. Qualitative micro CT analysis of FGF18 stimulated peri-implant bone formation. Schematic of a 0.6 x 5 mm titanium coated implant (yellow) superimposed on an X-ray of the mouse femur (**A**) showing its position in the femoral canal after inserting through the piriformis fossa of 8-10 month old male FGFR3$^{+/+}$ and FGFR3$^{-/-}$ mice. Femora harvested at 6 weeks post implantation and subjected to micro CT analysis revealed significant bone apposition in a 30 µm ring around the implant in 2D sections (**B**,**C**). 3D reconstructions of the ROI are shown for FGFR3$^{+/+}$ (**D**, **F**) and FGFR3$^{-/-}$ (**E**, **G**) femora. Treatment of the femoral canal with a single, 0.5 µg intra-operative dose of FGF18 resulted in more peri-implant bone in both FGFR3$^{+/+}$ (**F**) and FGFR3$^{-/-}$ (**G**) femora, than in the contralateral femora treated with PBS (**D**, **E**).

MSC isolation and FGF18 stimulation

Whole bone marrow was extracted from the tibiae and femora of 10 to 12 month old FGFR3$^{+/+}$ and FGFR3$^{-/-}$ mice and the MSC isolated by adherence to plastic as described previously (Valverde-Franco *et al.*, 2004). MSC harvested from three FGFR3$^{+/+}$ and three FGFR3$^{-/-}$ mice were used for each assay and culture media were replenished every 3 days. After removing the non-adherent cells on day 3, the adherent population was expanded for an additional 6 days before being trypsinized and seeded at a density of $5x10^4$ cells/cm^2 in 24-well plates, to assess proliferation, metabolic activity and differentiation. For proliferation, cells were harvested from quadruplet wells and counted after 3, 6 and 9 days of culture in alphaMEM (Minimal Essential Medium) with 2 % fetal bovine serum (FBS) (control) or control medium with 10^{-8} or 10^{-10}M FGF18. For differentiation, at 75 % confluence the medium was supplemented with 10 mM β-glycerophosphate, 50 µg/mL ascorbic acid and 2 % FBS (control) or supplemented medium with 10^{-8} or 10^{-10} M FGF18. After 6, 9 or 12 days, quadruplet wells were fixed in 4 % paraformaldehyde for 10 min and stained for ALP activity as described previously (Henderson *et al.*, 2000). The stained plates were scanned at a resolution of 2400 dpi (V350, Epson America, Long Beach, CA, USA.) and high quality 16-bit TIFF images analyzed using the Color Inspector plugin of ImageJ software (Version 1.43, Research Service Branch, NIH, Bethesda, MD, USA). Metabolic activity was assessed in triplicate at 3, 6 and 9 days using the Alamar Blue reagent according to the manufacturer's directions (Life Technologies, Carlsbad, CA, USA). At the end of the incubation period, replicate aliquots of medium were pipetted into the wells of a 96 well plate and the OD read on a Trek Diagnostic Systems (Cleveland, OH, USA) plate reader.

Statistical analyses

Quantitative *in vivo* data is expressed as the mean ± standard deviation (SD) of 5 FGFR3$^{+/+}$ and 9 FGFR3$^{-/-}$ biological replicates. Quantitative *in vitro* data was obtained from 3 biological replicates and 3-4 wells. All *in vivo* and *in vitro* data were assessed for normalcy using the Kolmogorov-Smirnov test. Comparisons between groups with normal distribution were performed with a Student's *t*-test and one-way analysis of variance, with *post-hoc* analysis performed using Tukey's honest significance difference when necessary. Comparisons between groups lacking normal distribution were performed with the Kruskal-Wallis one-way analysis of variance and Mann-Whitney U test. A Bonferroni correction was applied to the critical *p* value, which was initially set at 0.05, where applicable.

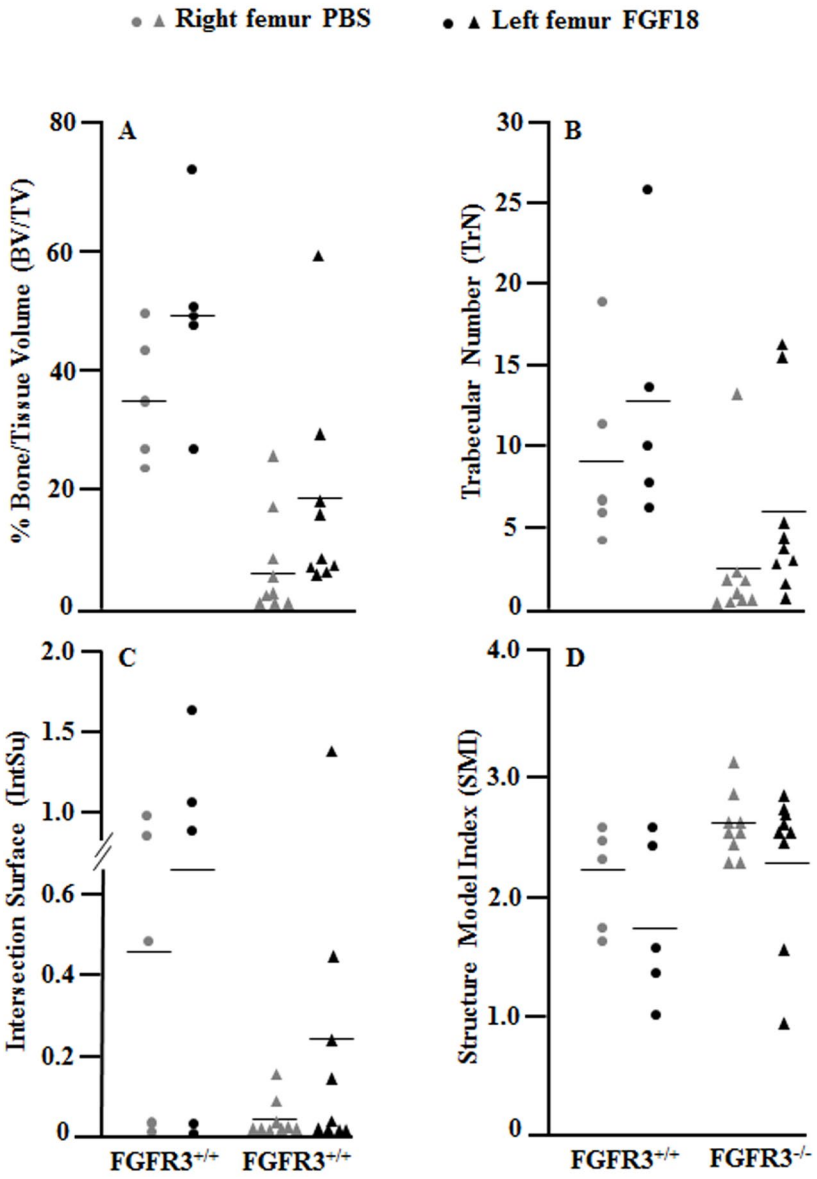

Fig. 2. Quantitative micro CT analysis of FGF18 stimulated peri-implant bone formation. New bone surrounding the implants in the 2 mm x 30 µm ROI shown in Fig 1A was quantified in PBS treated (grey) and FGF18 treated (black) femora of 5 $FGFR3^{+/+}$ (circles) and 9 $FGFR3^{-/-}$ (triangles) mice using the Skyscan proprietary software CTAn 2.0.0.1. Scatter plots with mean values (line) are shown for percent Bone Volume relative to Tissue Volume (**A**), Trabecular Number (**B**), Intersection Surface (**C**), which is the point of contact between the implant and newly formed bone and the Structure Model Index (**D**), which is an index of the plate/rod like structures in trabecular bone. Significant differences in BV/TV ($p < 0.002$), TrN ($p < 0.03$) IntSur ($p < 0.01$) and SMI ($p < 0.05$) in the right PBS treated femora of $FGFR3^{+/+}$ (circles) compared with $FGFR3^{-/-}$ (triangles) mice. Treatment of the left femur of $FGFR3^{-/-}$ mice with 0.5 µg FGF18 resulted in improvement in all parameters, which reached significance for BV/TV ($p < 0.02$) and TbN ($p < 0.01$). No significant differences were seen between left (FGF18) and right (PBS) femora in $FGFR3^{+/+}$ mice.

Results

Micro CT assessment of FGF18 stimulated bone regeneration

Micro CT imaging was used to quantify bone regeneration around the biocompatible implants in the femoral metaphysis of all specimens, as shown in schematic form in Fig. 1A. One of 400 two dimensional images taken from around the mid-point of the 2 mm region of interest (ROI), at low (Fig. 1B) and high (Fig. 1C) magnification, show the relationship between the 30 µm peri-implant bone ring and the existing cortical and trabecular bone. Three-dimensional reconstructions of the 400 images revealed more peri-implant bone in the femora treated with FGF18 (F, G) compared with those treated with PBS (Fig. 1D, E) in both $FGFR3^{+/+}$ (Fig. 1D, F) and $FGFR3^{-/-}$ (Fig. 1E, G) mice. Fig. 2 shows individual micro CT data for bone volume relative to total tissue volume (BV/TV), trabecular number (TbN), bone/implant intersection surface (IntSu) and architecture, measured as structure model index (SMI), for the left (FGF18) and right (PBS) femora of the five $FGFR3^{+/+}$ (circles) and nine $FGFR3^{-/-}$ (triangles) mice. In $FGFR3^{+/+}$ (circles) mice, there were no significant differences in the quantity or quality of bone in the right femur treated with PBS and the left femur treated with FGF18. In $FGFR3^{-/-}$ mice (triangles), treatment of the femoral canal with a single intra-operative dose of 0.5 µg of FGF18 resulted in significantly higher BV/TV ($p < 0.02$) and an increase in the number of trabeculae ($p < 0.01$) compared with the control femur treated with PBS. Comparisons made between the PBS-treated femora of $FGFR3^{+/+}$ (circles) and $FGFR3^{-/-}$ (triangles) mice revealed significant differences in BV/TV ($p < 0.002$), TrN (0.03) and IntSu (0.01). Comparison of data for the contra-lateral femur treated with FGF18 showed a reduction in the discrepancy between $FGFR3^{+/+}$ and $FGFR3^{-/-}$ bone volume (BV/TV $p < 0.01$) and abrogation of the differences in the TrN and IntSu.

Histological assessment of FGF18 stimulated bone regeneration

Un-decalcified bone specimens from $FGFR3^{+/+}$ and $FGFR3^{-/-}$ mice were embedded in PMMA and trimmed in the sagittal or horizontal plane to the mid-region of the

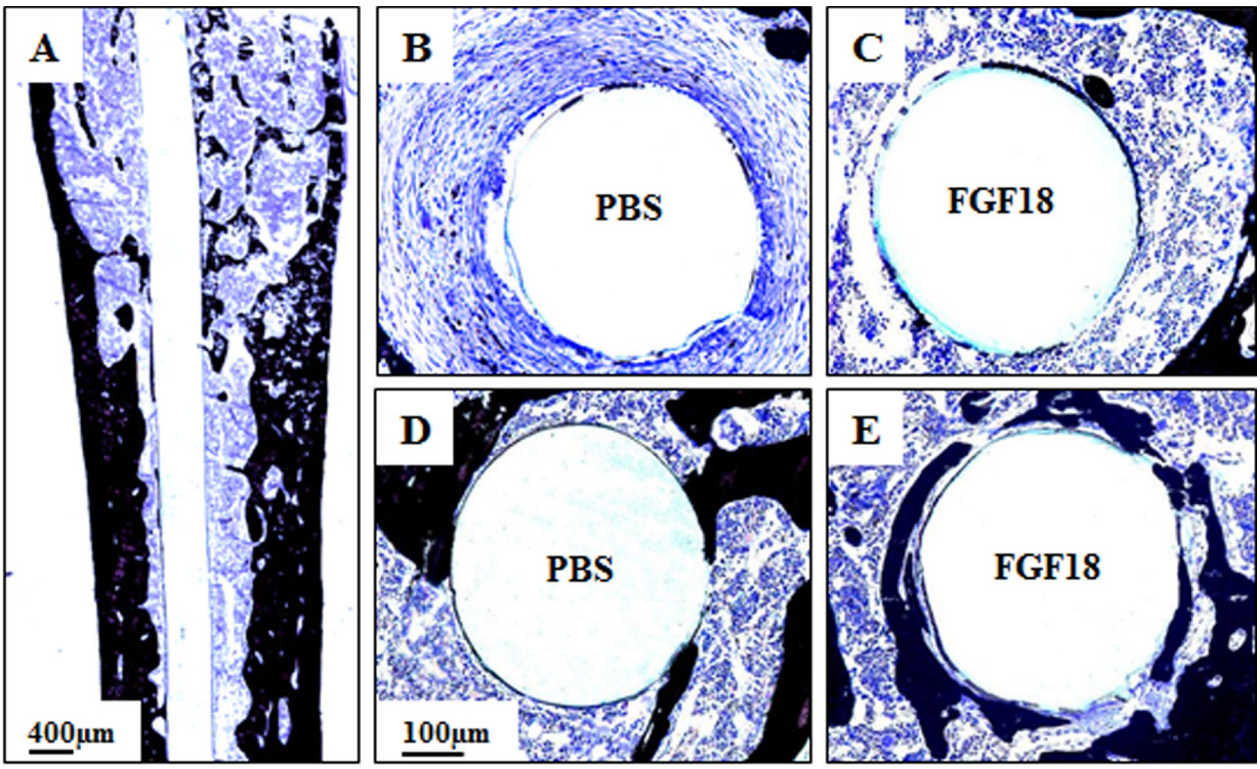

Fig. 3. Histological analysis of FGF18 stimulated peri-implant bone in FGFR3$^{-/-}$ mice. To further examine the tissue response to FGF18 in FGFR3$^{-/-}$ mice, femora were fixed in 4 % paraformaldehyde, embedded in polymethylmethacrylate (PMMA) and 5 μm sections cut in the sagittal (**A**) and transverse (**B-E**) planes. Under low power magnification (x 2.7) trabecular bone was seen apposed to the implant in the metaphyseal region of the femur (**A**). Transverse sections (x 20) from one mouse reveal a thick ring of fibrous tissue surrounded the implant in the PBS treated femur (**B**) and little bone but normal marrow in the contra-lateral FGF18 treated femur (**C**) The PBS treated femur of another mouse (**D**) showed normal marrow and bone but with a significant increase in bone in the FGF18 treated contra-lateral femur (**E**).

implant before harvesting 6 consecutive 5 μm sections for histochemical staining. Consistent with the micro CT data, von Kossa stained sections from the femora of FGFR3$^{+/+}$ (data not shown) and FGFR3$^{-/-}$ mice revealed more peri-implant bone in FGF18 treated left femora compared with the contra-lateral PBS treated right femora. Representative images of von Kossa stained sections from FGFR3$^{-/-}$ mice are shown in Fig. 3. A sagittal section (Fig. 3A) shows sparse trabeculae and little bone apposition to the implant while higher magnification images of transverse sections of FGFR3$^{-/-}$ femora revealed one of two general patterns shown in the upper (Fig. 3B, C) and lower (Fig. 3D, E) panels. In some mice, the femur treated with PBS exhibited a thick peri-implant ring of fibrous tissue (Fig. 3 B) and normal marrow with minimal bone in the FGF18 treated femur (Fig. 3 C). In others, the PBS treated femur looked similar to those of FGFR3$^{+/+}$ mice with peri-implant bone and normal cellular marrow, but significantly more bone apposed to the implant in the FGF18 treated contra-lateral femur (Fig. 3 E). Fig. 4 shows serial sections cut through the PBS treated (Fig. 4B, D, F) and FGF18 treated (Fig. 4A, C, E) femora of a third FGFR3$^{-/-}$ mouse, stained with von Kossa and toluidine blue (Fig. 4A, B), or for ALP to show osteoblasts (Fig. 4C, D) or tartrate-resistant acid phosphatase (TRAP) to show osteoclasts (Fig. 4E, F). The increase in peri-implant bone in the FGF18 treated femora (Fig. 4B) was accompanied by decreased and more focused ALP staining (Fig. 4D) and no apparent change in TRAP (Fig. 4F) compared with the PBS treated femur.

Ex vivo response of FGFR3$^{+/+}$ and FGFR3$^{-/-}$ MSC to FGF18

From the *in vivo* data it was evident that FGF18 promoted peri-implant bone formation in association with an apparent reduction in ALP activity. This occurred in the absence of any significant change in osteoclast activity, which is normally linked to osteoblast activity during bone metabolism, in TRAP positive cells. Working on the hypothesis that FGF18 influenced the terminal differentiation of osteoblasts into mineralizing cells we conducted *ex vivo* studies on bone marrow stromal cells (MSC) isolated from the long bones of FGFR3$^{+/+}$ and FGFR3$^{-/-}$ mice. Fig. 5 shows data from *ex vivo* mitogenic (top panel), metabolic (middle panel) and differentiation (bottom panel) assays. In the upper panels, after 9 days FGFR3$^{+/+}$ cells showed a small increase in cell numbers in response to 10^{-10} M FGF18 (hatched bars) and 10^{-8} M FGF18 (stippled bars), while the response of FGFR3$^{-/-}$ cultures was evident at 6 d and significantly greater at 9 d. The conversion of Alamar Blue reagent to fluorescent

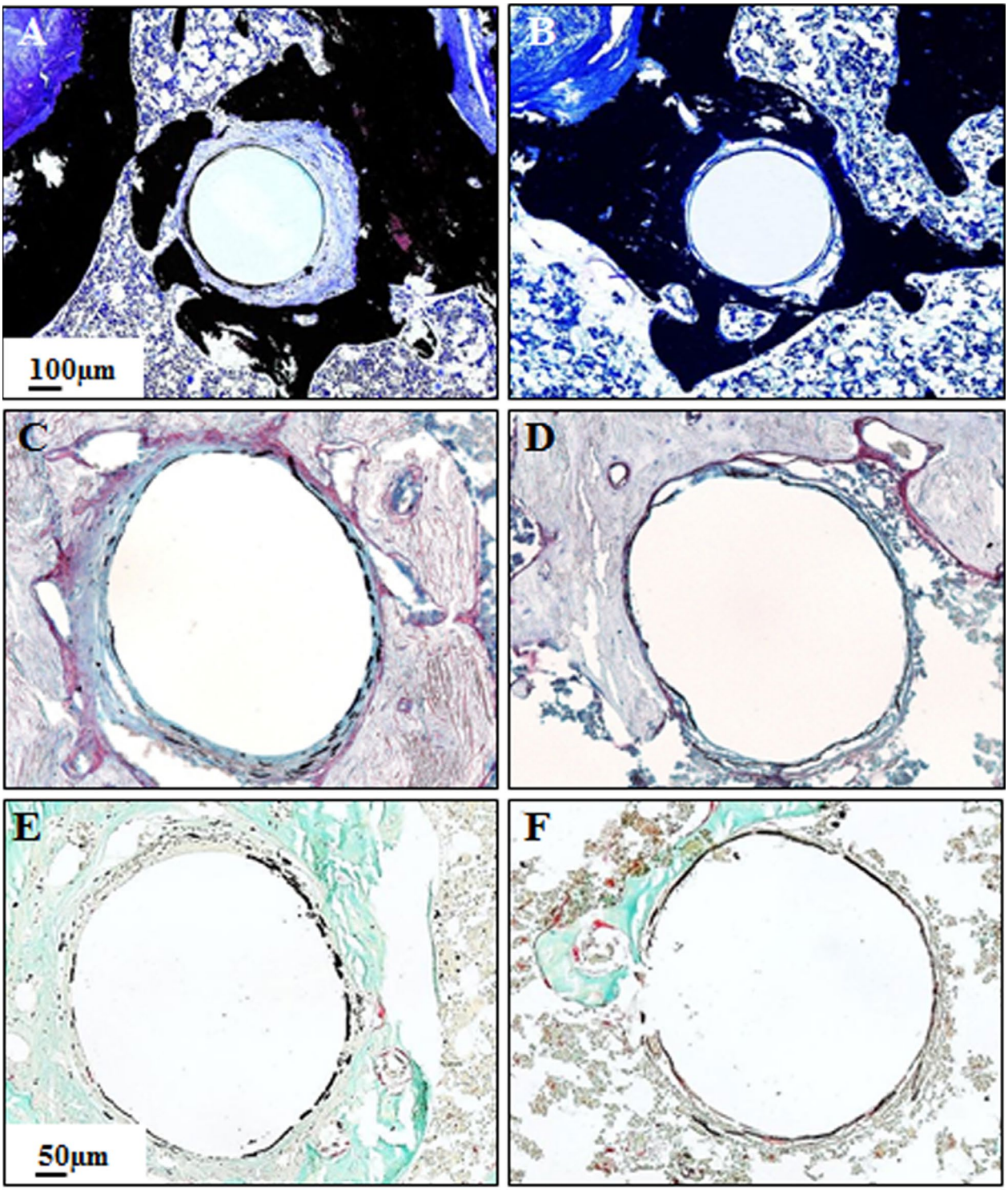

Fig. 4. Bone cell activity in FGF18 and PBS treated femora of FGFR3$^{-/-}$ mice. 5 µm transverse sections were cut in the 2 mm ROI from the left (0.5 µg FGF 18) and right (PBS control) femora of an FGFR3$^{-/-}$ mouse and stained with Von Kossa/Toluidine Blue to show morphology (**A**, **B**), alkaline phosphatase (ALP) for osteoblasts (**C**, **D**) and tartrate resistant acid phosphatase (TRAP) for osteoclasts (**E**, **F**). The PBS treated femora exhibited a peri-implant ring of fibrous tissue (**A**), more ALP activity (**C**) and similar TRAP activity (**E**) compared to the FGF18 treated femur.

pink during cellular metabolism was modestly increased by addition of FGF18 at either concentration to both FGFR3$^{+/+}$ and FGFR3$^{-/-}$ cells compared with control cells cultured in 2 % FBS. Normalization of the D9 Alamar Blue data to account for the increase in cell numbers in response to 10^{-10} M FGF18 and 10^{-8} M FGF18 respectively revealed reductions of 14 % and 21 % in FGFR3$^{+/+}$ cells and 42 % and 52 % in FGFR3$^{-/-}$ cells. Normalization of the corresponding ALP data revealed effective reductions of 43 % and 73 % in FGFR3$^{+/+}$ cells and 77 % and 74 % in FGFR3$^{-/-}$ cells.

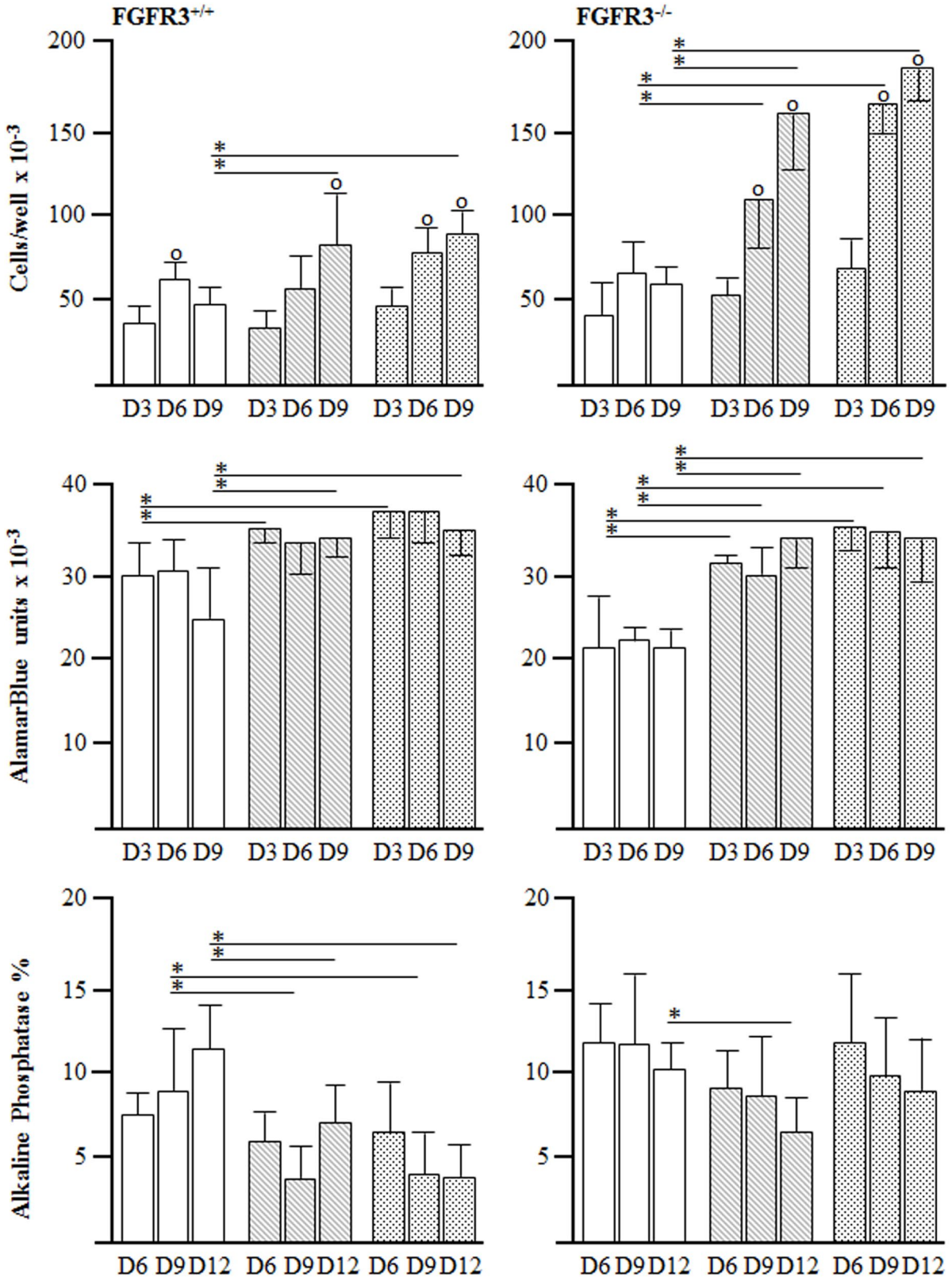

Fig 5. *Ex Vivo* response of FGFR3$^{+/+}$ and FGFR3$^{-/-}$ MSC to FGF18. MSC isolated from bone marrow harvested from the tibiae and femora of 10-12 month old FGFR3$^{+/+}$ and FGFR3$^{-/-}$ mice were plated at 50,000 cells/cm^2 in 24 well plates and grown in the presence of 2 % FBS (white bars), 2 % FBS + 10^{-10} M (hatched bars) or 10^{-8} M (stippled bars) FGF18. Quadruplet wells were harvested at the indicated times for assessment of proliferation (**A**), metabolic activity (**B**) or differentiation (**C**). Time dependent increases in cell numbers were seen in cultures of FGFR3$^{+/+}$ and FGFR3$^{-/-}$ cells (o). Addition of 10^{-10} M FGF18 or 10^{-8} M FGF18 elicited a further increase compared with 2 % serum alone (*), with a significantly more robust response in FGFR3$^{-/-}$ cultures. Metabolic activity was stimulated by FGF18 in cultures of FGFR3$^{+/+}$ and FGFR3$^{-/-}$ cells whereas ALP activity was marginally decreased. The results are representative of 3 biological replicates and are expressed as the mean ± SD of four wells for each time point for each assay.

Discussion

Age-related changes in skeletal cell function lead to poor quality bone and a reduction in the capacity for regeneration, which impact negatively on the fixation strength and long term viability of joint replacements (Lee and Goodman, 2008). It is estimated that up to 70 % of the individual differences in bone cell function are influenced by heritable factors, including the availability of skeletal growth factors to support bone regeneration. There is an extensive literature, reviewed by Ornitz and Marie (Ornitz and Marie, 2002) that characterizes the skeletal phenotypes associated with activating mutations in FGF receptors, which result in short limbed dwarfism and/or cranial synostosis. Mouse models of these disorders, generated by targeted disruption of the genes encoding proteins essential for skeletal cell proliferation, maturation and function, have been instrumental in building knowledge of potential therapeutic targets to promote regeneration and repair of the ageing skeleton. Examples from our own work include characterization of the cartilage and bone phenotypes of adult $FGFR3^{-/-}$ mice, which exhibit defects in articular cartilage metabolism that lead to early onset osteoarthritis and bone defects similar to those seen in the ageing human skeleton (Valverde-Franco *et al.*, 2004; Valverde-Franco *et al.*, 2006). *Ex vivo* analysis of chondrogenesis and cartilage formation by MSC released from the limb buds of fetal $FGFR3^{-/-}$ mice revealed defects in proliferation, differentiation, and matrix production that were refractory to treatment with FGF18 and resulted in altered expression of FGFR1 and FGFR2 (Davidson *et al.*, 2005). FGF18 treatment of primary articular chondrocytes increased their proliferation and matrix production, as well as up-regulating expression of FGFR2 and FGFR3 (Ellsworth *et al.*, 2002). Subsequently, FGF18 was shown to induce cartilage regeneration and repair in a rat model of osteoarthritis induced by meniscal injury (Moore *et al.*, 2005). Others have shown that pharmacologic inhibition of signaling downstream of a constitutively active FGFR2 in genetically modified mice resulted in reversal of craniosynostosis and normal development of the cranial vault (Eswarakumar *et al.*, 2006). Targeted inactivation of the mouse gene encoding FGF18 had a similar effect in delaying intramembranous ossification, which suggested it might be a ligand for FGFR2 in the developing skull (Liu *et al.*, 2002; Ohbayashi *et al.*, 2002). The remainder of the skeleton of FGF18-deficient mice looked remarkably similar to that of mice in which FGFR3 had been inactivated. Taken together, these studies have identified FGF18 as a critical ligand for FGFR3 and FGFR2 in areas of the skeleton undergoing endochondral and intramembranous ossification, as well as a potential therapeutic agent for adult cartilage repair. The objective of the current study was to determine if local administration of recombinant FGF18 could enhance bone regeneration and fixation of a biocompatible implant in the femoral canal of osteopenic $FGFR3^{-/-}$ mice using $FGFR3^{+/+}$ mice as a control.

In previous work, quantitative micro CT analysis of the distal femur and lumbar vertebrae of 4 month old $FGFR3^{-/-}$ mice revealed a reduction in trabecular and cortical bone, in association with disorganized micro-architecture, compared with $FGFR3^{+/+}$ mice (Valverde-Franco *et al.*, 2004). In the current study, a similar, although more pronounced reduction in trabecular bone was documented in the peri-implant tissue of the proximal metaphysis of PBS treated femora in the 8-10 month old $FGFR3^{-/-}$ mice. Whereas normal marrow and bone apposed the flexible implant in $FGFR3^{+/+}$ mice, a thick ring of peri-implant fibrous tissue was frequently seen in the $FGFR^{-/-}$ mice, which indicated a fundamental difference in the response of the intra-medullary cells to a "foreign body". Treatment of the contra-lateral femur with FGF18 resulted not only in a significant increase in peri-implant bone and an improvement in its architecture, but also abrogation of the peri-implant fibrous response seen in the $FGFR3^{-/-}$ mice. Fibrous overgrowth is proposed to be the end product of a chronic inflammatory response to a foreign body and poses a major barrier to the integration and biological performance of medical devices such as prostheses, implantable biosensors and drug delivery devices (Bauer and Schills, 1999; Wu and Grainger, 2006). The fibrous response to implanted materials has been shown to involve the ubiquitous matrix protein fibronectin, which binds to heterodimeric integrin cell surface receptors (Keselowsky *et al.*, 2007). In previous work we showed that alpha 5 integrin was down-regulated in chondrogenic cells expressing $FGFR3^{Ach}$, carrying the activating achondroplasia mutation and that beta 1 integrin expression was up-regulated by FGF18 in $FGFR3^{+/+}$ cultures of limb bud MSC, but was undetectable in $FGFR3^{-/-}$ cells (Davidson *et al.*, 2005; Henderson *et al.*, 2000). The changes in integrin expression were manifested in altered adhesion of the cells to fibronectin and collagen substrates and provided evidence for a functional, albeit complex, relationship between FGF signaling and cell-substrate interactions. In this context, it was recently demonstrated that the absence of plasma fibronectin in mice resulted in a two-fold increase in fibrous tissue surrounding sub-cutaneous polyethylene implants (Keselowsky *et al.*, 2007) thus implicating fibronectin in the fibrous response of a host to foreign bodies. It is therefore possible that the increased fibrous response to implants in $FGFR3^{-/-}$ mice was related to altered recognition of fibronectin by bone marrow MSC and that the defect was reversed by FGF18 treatment. Additional longitudinal studies that measure inflammatory cytokine production and the expression patterns of integrins on the surface of $FGFR3^{+/+}$ and $FGFR3^{-/-}$ MSC exposed to different substrata in the presence and absence of FGF18 are needed for clarification of the molecular mechanisms underlying the anomalous fibrous response of $FGFR3^{-/-}$ mice to intra-femoral implants.

The FGF18-stimulated increase in the quantity and quality of bone surrounding the non-load bearing implant in the absence of FGFR3 signaling suggested the effect was mediated by FGFR1 or FGFR2, which are also expressed in skeletal cells. A comprehensive analysis of FGF and FGFR gene expression, using quantitative PCR, was undertaken to examine the relative levels of expression during the early and late stages of healing in a mouse model of tibial fracture with internal fixation (Schmid *et al.*, 2009). FGFR3 and FGF18 both peaked after 9 days of healing, along with recognized markers of chondrogenesis. This

was in contrast to FGFR1 and 2, which continued to rise throughout the 14-day timeframe, along with osteogenic markers. Although the fracture model differs significantly from the current study in a number of respects, including mice aged 8 weeks *vs.* 40 week old mice, fracture repair *vs.* implant fixation and tibia *vs.* femur, the results support the hypothesis that FGF18 could mediate its osteogenic effect through FGFR1 or 2, rather than FGFR3. In addition to promoting intramembranous ossification via FGFR2 in calvarial bone, FGF18 has been shown to stimulate the differentiation of MSC into osteoblasts through an autocrine mechanism involving activation of FGFR1 or FGFR2 and signaling through the PI3K pathway (Hamidouche *et al.*, 2010). Furthermore, conditional inactivation of a PI3K signaling repressor (PTEN) in the perichondrium of developing mouse limbs resulted in an increase in the populations of osteoprogenitor cells and osteoblasts, with a concomitant increase in bone, most likely mediated through FGFR2 (Guntur *et al.*, 2011). Although both FGFR1 and FGFR2 have been identified as potential mediators of the osteogenic response of MSC to FGF18, most of the data suggest FGFR2 is the primary target. This includes surface plasmon resonance studies of the binding affinity of FGF18 to different splice forms of FGFR1 and FGFR2 (Olsen *et al.*, 2006) and biochemical studies investigating the receptor specificity of the family of FGF ligands in mitogenic assays (Zhang *et al.*, 2006).

In our previous work that characterized the bone phenotype of 4-month old FGFR3$^{-/-}$ mice, increased staining for alkaline phosphatase activity was seen in the growth cartilage and cells lining bone trabeculae compared with that seen in the FGFR3$^{+/+}$ mice. This was associated with a significant reduction in calcein labeling of actively mineralizing surfaces and large cuboidal osteoblasts adjacent to wide osteoid seams (Valverde-Franco *et al.*, 2004). In the current study, ALP was also increased in FGFR3$^{-/-}$ femora treated with PBS and appeared as a diffuse band of staining outside of the fibrous ring of tissue surrounding the implant. In the contra-lateral FGF18 treated femur ALP was significantly reduced and appeared as a well-defined line of staining adjacent to the implant and surrounding bone. The increase in mineralized tissue thus correlated with an apparent reduction in activity of the enzyme that breaks down inorganic pyrophosphate, which serves a dual role as a major inhibitor of tissue mineralization and the source of phosphate that combines with calcium to form hydroxyapatite mineral (Hessle *et al.*, 2002). Treatment of FGFR3$^{-/-}$ bone-marrow derived MSC *ex vivo* with FGF18 appeared to stimulate their metabolic activity, and to have little effect on ALP activity, as shown previously (Valverde-Franco *et al.*, 2004). However, when the data was normalized to the increase in cell numbers, there was effectively a 50 % reduction in metabolism and 75 % reduction in ALP. Taken together with the *in vivo* data, this suggests the cells had reached confluence and initiated mineralization earlier than they would have in the absence of FGF18. This interpretation of the data is also consistent with that of others who used an RNAi-based approach to demonstrate that targeted down-regulation of metabolic pathways in myoblasts led to their differentiation into myotubules (Bracha *et al.*, 2010). A similar approach using MSC to target enzymes such as TNAP, PHOSPHO-1, PC-1 and ANK would provide valuable information that could be used to develop therapeutic interventions for disorders related to excessive or insufficient mineralization (Golub and Boesze-Battaglia, 2007; McGraw and Mittal, 2010).

In summary, we have shown that a single intra-operative dose of FGF18 reduced marrow fibrosis and stimulated bone formation around a titanium-coated femoral implant in aged FGFR3$^{-/-}$ mice and that the effect was most likely mediated by FGFR2. The results of this pre-clinical study suggest that FGF18 could be used in the clinical setting to promote integration of orthopedic hardware in poor quality bone.

Acknowledgements

The authors gratefully acknowledge the kind gift of FGFR3$^{+/-}$ founder mice from Dr D.M. Ornitz at Washington University, from which the McGill colony was established. The mouse implants were micro-fabricated at the McGill Institute for Advanced Materials (MIAM) in consultation with Dr S. Vengallatore, G Sosale and M. Nanini, and B. ElCharaani provided valuable assistance with the *in vitro* studies. This work was supported by grants from the Canadian Institutes of Health Research (CIHR) and by the Fonds de recherche en santé du Québec (FRSQ)-sponsored Réseau de recherche en santé buccodentaire et osseuse (RSBO). AC and CG were supported by fellowships from FRSQ, RSBO, CIHR-MENTOR and the Research Institute of the McGill University Health Centre (RI-MUHC), which is funded by an FRSQ Center grant.

References

Bauer T, Schills J (1999) The pathology of total joint arthroplasty: Part 1, mechanisms of implant fixation. Skeletal Radiol **28**: 423-432.

Bracha AL, Ramanathan A, Huang S, Ingber D, Schreiber SL (2010) Carbon metabolism-mediated myogenic differentiation. Nature Chem Biol **6**: 202-204.

Colvin JS, Bohne BA, Harding GW, McEwen DG, Ornitz DM (1996) Skeletal overgrowth and deafness in mice lacking fibroblast growth factor receptor 3. Nature Genet **12**: 390-397.

Davidson D, Blanc A, Filion D, Wang H, Plut P, Pfeffer G, Buschmann M, Henderson JE (2005) FGF18 signals through FGFR3 to promote chondrogenesis. J Biol Chem **280**: 20509-20515.

Egermann M, Goldhahn J, Schneider E (2005) Animal models for fracture treatment in osteoporosis. Osteoporosis Int **16**: S129-S138.

Ellsworth JL, Berry J, Bukowski T, Claus J, Feldhaus A, Holderman S, Holdren MS, Lum KD, Moore EE, Raymond F, Ren H, Shea P, Sprecher C, Storey H, Thompson DL, Waggie K, Yao L, Fernandest RJ, Eyre DR, Hughes SD (2002) Fibroblast growth factor-18 is a trophic factor for mature chondrocytes and their progenitors. Osteoarthritis Cartilage **10**: 308-320.

Eswarakumar V, Ozcan F, Lew ED, Bae JH, Tome F, Booth CJ, Adams DJ, Lax I, Schlessinger J (2006) Attenuation of signaling pathways stimulated by pathologically activated FGF-receptor 2 mutants prevents craniosynostosis Proc Natl Acad Sci USA **103**: 18603-18608.

Eswarakumar V, Schlessinger J (2007) Skeletal overgrowth is mediated by deficiency in a specific isoform of fibroblast growth factor receptor 3. Proc Natl Acad Sci USA **104**: 3937-3942.

Gao C, Seuntjens J, Kaufman GN, Tran-Khan N, Butler A, Li A, Wang H, Buschmann MD, Harvey EJ, Henderson JE (2012) Mesenchymal stem cell transplantation to promote bone healing. J Orthop Res **30**: 1183-1189.

Golub E, Boesze-Battaglia K (2007) The role of alkaline phosphatase in mineralization. Curr Opin Orthop **18**: 444-448.

Guntur AR, Reinhold MI, Cuellar J, Naski MC (2011) Conditional ablation of Pten in osteoprogenitors stimulates FGF signaling. Development **138**: 1433-1444.

Hacking SA, Zuraw M, Harvey EJ, Tanzer M, Krygier JJ, Bobyn JD (2007) A physical vapor deposition methods for controlled evaluation of biological response to biomaterial chemistry and topography. J Biomed Mater Res **82A**: 179-187.

Hamidouche Z, Fromigue O, Nuber U, Vaudin P, Pages J, Ebert R, Jakob F, Miraoui H, Marie P (2010) Autocrine fibroblast growth factor 18 mediates dexamethasone-induced osteogenic differentiation of murine mesenchymal stem cells. J Cell Physiol **224**: 509-515.

Henderson JE, Naski MC, Aarts M, Wang D, Cheng L, Goltzman D, Ornitz DM (2000) Expression of FGFR3 with the G380R achondroplasia mutation inhibits proliferation and maturation of CFK2 chondrocytic cells. J Bone Miner Res **15**: 155-165.

Hessle L, Johnson KA, Anderson HC, Narisawa S, Sali A, Goding JW, Terkeltaub R, Millan JL (2002) Tissue nonspecific alkaline phosphatase and plasma cell membrane glycoprotein-1 are central antagonistic regulators of bone mineralisation. Proc Natl Acad Sci USA **99**: 9445-9449.

Junker R, Dimakis A, Thoneick M, Jansen J (2009) Effects of implant surface coatings and composition on bone integration: a systematic review. Clin Oral Impl Res **20 S4**: 185-206.

Keselowsky B, Bridges AW, Burns KL, Tate CC, Babanesee JE, LaPlaca MC, Garcia AJ (2007) Role of plasma fibronectin in the foreign body response to bimaterials. Biomaterials **28**: 3626-3631.

Lee K, Goodman SB (2008) Current state and future of joint replacements in the knee and hip. Expert Review of Medical Devices **5**: 383-393.

Liu Z, Xu J, Colvin JS, Ornitz DM (2002) Coordination of chondrogenesis and osteogenesis by fibroblast growth factor 18. Genes Dev **16**: 859-869.

Liu Z, Lavine KJ, Hung IH, Ornitz DM (2007) FGF18 is required for early chondrocyte proliferation, hypertrophy and vascular invasion of the growth plate. Dev Biol **302**: 80-91.

McGraw T, Mittal V (2010) Stem cells: metabolism regulates differentiation. Nature Chem Biol **6**: 176-177.

Moore EE, Bendele AM, Thompson DL, Littau A, Waggie KS, Reardon B, Ellsworth J (2005) Fibroblast growth factor-18 stimulates chondrogenesis and cartilage repair in a rat model of injury-induced osteoarthritis. Osteoarthritis Cartilage **13**: 623-631.

Nauth A, Miclau T, Bhandari M, Schemitsch E (2011) Use of osteobiologics in the management of osteoporotic fractures. J Orthop Trauma **25**: S51-55.

Ohbayashi N, Shibayama M, Kurotaki Y, Imanishi M, Fujimori T, Itoh N, Takada S (2002) FGF18 is required for normal cell proliferation and differentiation during osteogenesis and chondrogenesis. Genes Dev **16**: 870-879.

Olsen SK, Li JY, Bromleigh C, Eliseenkova A, Ibrahimi O, Lao Z, Zhang F, Linhardt RJ, Joyner A, Mohammadi M (2006) Structural basis by which alternative splicing modulates the organizer activity of FGF8 in the brain. Genes Dev **20**: 185-198.

Ornitz DM, Marie PJ (2002) FGF signaling pathways in endochondral and intramembranous bone development and human genetic disease. Genes Dev **16**: 1446-1465.

Schmid G, Kobayashi C, Sandell L, Ornitz DM (2009) Growth factor expression during skeletal fracture healing in mice. Dev Dynamics **238**: 766-774.

Valverde-Franco G, Lui H, Davidson D, Chai S, Valderrama-Carvajal H, Goltzman D, Ornitz DM, Henderson JE (2004) Defective bone mineralization and osteopenia in young adult FGFR3-/- mice. Hum Mol Genet **13**: 271-284.

Valverde-Franco G, Binette JS, Li W, Wang H, Chai S, Laflamme F, Tran-Khahn N, Quenneville E, Meijers T, Poole AR, Mort JS, Buschmann MD, Henderson JE (2006) Defects in articular cartilage metabolism and early arthritis in fibroblast growth factor receptor 3 deficient mice. Hum Mol Genet **15**: 1783-1792.

Wu P, Grainger DW (2006) Drug/device combinations for local drug therapies and infection prophylaxis. Biomaterials **27**: 2450-2467.

Zhang X, Ibrahimi OA, Olsen SK, Umemori H, Mohammadi M, Ornitz DM (2006) Receptor specificity of the fibroblast growth factor family. J Biol Chem **281**: 15694-15702.

Discussion with Reviewers

Reviewer I: The FGF18 is injected into the medullar canal. It is not clear whether the injected FGF18 stays locally or is distributed to other body locations. In view of this, there is also no information about the final required concentration to achieve activity of tissue formation. Further, it is unclear what the local effect of the FGF18 is (what is the working mechanism?).

Authors: The point about leakage of FGF18 from the site of injection is valid. The short answer is we do not know as it would require a dedicated series of experiments, beyond the scope of the current study, to track labeled protein using histological analyses at timed intervals after insertion of the rod. We used a supra-physiological dose of FGF18, to account for loss by dispersal or degradation, which did in fact elicit a statistically significant anabolic response in 9 FGFR3-/- mice. We propose in paragraphs

one and four of the discussion the potential high affinity binding partners for FGF18 that might have mediated its anabolic effect in bone.

Regarding the related question of the final concentration required for bone tissue formation, once again the short answer is that we do not know. To date there is no published literature on the impact of FGF18 treatment on cells of the osteogenic lineage *in vivo*. Our experiments were therefore designed after those published by J.L. Ellsworth (Ellsworth *et al*., 2002; Moore *et al*., 2005 (additional references) as well as references in those papers), investigating the impact of recombinant FGF18 on chondrogenesis and cartilage repair in rodent models. We also discussed the subject of dose response at great length with Christoph Ladel from Merck Serono, who supplied us with the recombinant protein, and with our colleague Dave Ornitz at Washington University, who has published extensively on the biochemical and physiological properties of FGFs and their receptor binding characteristics. Three major points were distilled from these consultations: (1) At a physiological pH, such as that found in the femoral canal, FGF18 has a net positive charge (isoelectric point > 9.0) that would most likely result in its strong affinity for the negatively charged proteoglycans on the marrow cells, (2) Dose-response experiments conducted *ex vivo* and *in vivo* in both mouse and rat indicated 5 μg was sufficient to elicit a strong anabolic response, (3) The anabolic effect of FGF18 was apparent in populations of both immature and mature chondrogenic cells. Working on the hypothesis that FGF18 would have a similar anabolic effect on osteoblasts and their precursors as on chondrocytes and their precursors we used a single 5 μg dose of FGF18 injected directly into the medullary canal.

Reviewer I: The "implants" are made of nylon. This is a flexible material. Usually, hard materials are used for bone implants. It is possible that the mechanical characteristics of the implant have an additional effect on bone formation. Please comment.

Reviewer II: What is the justification for the chosen implant? This is not described anywhere. Why was not a simple titanium wire chosen?

Authors: The assumption that the titanium coated intramedullary implant is more flexible than a solid titanium wire, for example, is correct. The model has been used previously in the lab and was recently published (Gao *et al*., 2012, text reference). The decision to use a flexible implant was based on 3 important points: (1) at the time the model was developed we could not cut serial 5 μm sections from the specimens with a solid titanium wire in blocks embedded in PMMA at low temperature to preserve enzyme histochemistry (ALP, TRAP), (2) adult FGFR mutant mice have a significant varus deformation of the femur (Valverde Franco *et al*., 2004, text reference), which frequently resulted in perforation of the fragile diaphysis when using solid titanium or metal alloy pins, (3) apart from the technical difficulties associated with inserting a 0.4 mm x 5 mm wire through the piriformis fossa into the femoral canal of a mouse, we had a more physiological reason for using flexible implants. The titanium coated nylon implant has an elastic modulus ~ 50 % that of bone whereas solid titanium is x 12 and stainless steel x 21 fold greater than bone. The lower modulus of elasticity would therefore increase the load transfer to bone, which would theoretically reduce the risk of stress shielding and increase peri-implant bone formation.

Additional References

Ellsworth JL, Berry J, Bukowski T, Claus J, Feldhaus A, Holderman S, Holdren MS, Lum KD, Moore EE, Raymond F, Ren H, Shea P, Sprecher C, Storey H, Thompson DL, Waggie K, Yao L, Fernandes RJ, Eyre DR, Hughes SD (2002) Fibroblast growth factor-18 is a trophic factor for mature chondrocytes and their progenitors. Osteoarthritis Cartilage **10**: 308-320.

Moore EE, Bendele AM, Thompson DL, Littau A, Waggie KS, Reardon B, Ellsworth JL (2005) Fibroblast growth factor-18 stimulates chondrogenesis and cartilage repair in a rat model of injury-induced osteoarthritis. Osteoarthritis Cartilage **13**: 623-631.